Available online at www.sciencedirect.com
SCIENCE DIRECT®
Radiation Physics and Chemistry 75 (2006) 473–478
Radiation Physics and Chemistry
www.elsevier.com/locate/radphyschem

Fluorescence detection of hydroxyl radicals

Gerald L. Newton[a], Jamie R. Milligan[b,*]

[a]Department of Chemistry, University of California at San Diego, 9500 Gilman Drive, La Jolla, CA 92093-0610, USA
[b]Department of Radiology, University of California at San Diego, 9500 Gilman Drive, La Jolla, CA 92093-0610, USA

Received 11 October 2005; accepted 26 October 2005

Abstract

The hydroxyl radical ($^{\bullet}$OH), a product of water radiolysis, reacts to hydroxylate aromatic organic compounds. In some cases, these hydroxylated products are fluorescent. Examples include the benzoate, coumarin, and phenoxazinone systems. For representative members of these systems, we have determined both the rate constants for reaction with $^{\bullet}$OH and the yields of the fluorescent products. The rate constants all fall in the range 2×10^9 to 2×10^{10} L mol^{-1} s^{-1}, and the yields 5–11% per $^{\bullet}$OH. These results suggest that it may prove feasible to construct a probe consisting of two groups both of which must react with $^{\bullet}$OH to become fluorescent. The efficient process of fluorescence resonance energy transfer implies that such a probe might be able to detect $^{\bullet}$OH clusters, which are generally assumed to be a characteristic feature of energy deposition by ionizing radiation.

Keywords: Fluorescence; Hydroxyl radical; Gamma irradiation

1. Introduction

It is generally accepted that the biological effects of ionizing radiation are a consequence of damage to DNA. Mechanisms by which this damage is formed are classified as the direct effect (ionization of the DNA itself), the quasi-direct effect (ionization of water molecules closely associated with the DNA which then react with it by electron transfer, and the indirect effect (Bernhard and Close, 2003). The indirect effect involves radiolysis of water to form diffusible and highly reactive intermediates, some of which react with the DNA target. The indirect effect makes a significant contribution to biologically significant DNA damage in biological systems. The hydroxyl radical ($^{\bullet}$OH) is the radical species largely responsible for DNA damage by the indirect effect.

Because of the importance of $^{\bullet}$OH, several different methods have been devised to detect it in various experimental systems (Gutteridge and Halliwell, 2000). These include spin traps which react with many short-lived radicals to form relatively stable species which may then be detected and characterized by EPR spectroscopy (Bottle et al., 2003). Inhibition of fluorescence quenching has also been applied to the detection of radical species (Li et al., 1997; Ivan and Scaiano, 2003; Soh et al., 2004). Unfortunately these methods are not particularly selective for $^{\bullet}$OH.

However, one characteristic feature of the chemical reactivity of $^{\bullet}$OH is the hydroxylation of aromatic rings (in the presence of a suitable additional oxidizing agent) (Lundqvist and Eriksson, 2000; Biondi et al., 2001). An example is the formation of phenol from benzene. In the case where the substrate is not benzene but instead a

*Corresponding author. Fax: +858 534 0265.
E-mail address: jmilligan@ucsd.edu (J.R. Milligan).

0969-806X/$ - see front matter © 2005 Elsevier Ltd. All rights reserved.
doi:10.1016/j.radphyschem.2005.10.011

benzoate, a coumarin, or a phenoxazinone, at least one of the hydroxylated products is highly fluorescent. These fluorescent products are respectively salicylates, umbelliferones, and resorufins. This property has found use as the basis of a sensitive assay for $^{\bullet}$OH (Manevich et al., 1997; Saran and Summer, 1999; Ali et al., 2000; Liu et al., 2002). In a slightly different form, it has also been used as an assay for the enzymes aryl hydrocarbon hydroxylase (Nakamura et al., 2001).

A distinctive feature of the spatial distribution of energy deposition by ionizing radiation is that it is non-uniform. Although $^{\bullet}$OH is a small and diffusible species, its lifetime under cellular conditions is relatively short, being in the nanosecond range. This corresponds to small diffusion distances of a few nanometers (Fulford et al., 2001). The spatial distribution of $^{\bullet}$OH on the time scale of its reaction with DNA therefore resembles the original track structure of the ionizing radiation. Although it is the reaction of $^{\bullet}$OH with DNA which is of importance in the biological effects of the indirect effect, evidence for non-uniform radical distributions producing clustered DNA damage is not easily obtained in model systems. Part of the difficulty derives from the reactivity of alkyl and alkylperoxyl radicals with DNA, either of which may lead to large artifactual yields of DNA damage (Milligan and Ward, 1994; Milligan et al., 1996). Simpler chemical systems have the potential to provide useful information about radical clustering at the nanometer level. This requires an assay system which is insensitive to single $^{\bullet}$OHs but responsive to multiple $^{\bullet}$OHs.

In principle, fluorescence detection of $^{\bullet}$OH may offer such a possibility, because of its potentially high selectivity and sensitivity. There are at least two methods by which this may be achieved. One involves the hydroxylation of an aromatic substrate which forms a fluorescent chromophore only after two −OH groups, have been introduced. Phenoxazine is an example of such a substrate, since the product formed by hydroxylation at both the 3- and 7-positions (7-hydroxy-3*H*-phenoxazin-3-one, also known by the trivial name of resorufin) is known to be fluorescent. Unfortunately, phenoxazine itself is insufficiently soluble in aqueous media to be useful. Moreover, as might be expected of an aromatic amine, it is sensitive to oxidation by species other than $^{\bullet}$OH (Villegas et al., 2005). Another example is the 9-phenylxanthene system, which after hydroxylation at both the 3- and 6-positions forms a fluorescein. In this case however, the monohydroxylated intermediate is also significantly fluorescent (Shen et al., 1995).

An alternative approach exploits the phenomenon of fluorescence resonance energy transfer (Selvin, 2000). A heterodimer consisting of (for example) a salicylate and an umbelliferone covalently linked to one another would tend to exhibit the property that excitation of the salicylate results in no detectable emission from it, because the energy is instead transferred from the salicylate (the donor) to the umbelliferone (the acceptor), resulting in an emission characteristic of the umbelliferone chromophore. Such intramolecular energy transfer is in general highly efficient (to the extent of being essentially quantitative) over distances of several nanometers, a distance of the same order as the expected diffusion distance of $^{\bullet}$OH. The mechanism involves coupling between diploes and not orbital overlap. Increasing coincidence of the emission spectrum of the donor and the excitation spectrum of the acceptor, higher extinction coefficients, and higher quantum yields all result in a more efficient and longer range interaction (Selvin, 2000; Watrob et al., 2003).

The sensitivity of a fluorescence assay for $^{\bullet}$OH depends upon additional factors. In addition to the usual concerns about the extinction coefficient and the quantum yield, it is also important to quantify the reactivity with $^{\bullet}$OH and the yield of the fluorescent product. There are multiple sites at which $^{\bullet}$OH may add to an aromatic ring system, most of which produce non-fluorescent products. In order to examine the feasibility of the approach discussed above, we have prepared derivatives of benzoic acid, coumarin, and phenoxazine. We have determined the yields in which the fluorescent products are formed from $^{\bullet}$OH, and the rate constants for these reactions.

2. Experimental

2.1. Preparation of 4-(acetylamino)benzoic acid (*1a*)

At room temperature, a solution of acetic anhydride (1.89 mL, 20 mmol) in acetonitrile (15 mL) was added from a dropping funnel to a mixture of 4-aminobenzoic acid (2.74 g, 20 mmol) and triethylamine (2.79 mL, 20 mmol) in acetonitrile (50 mL) and water (25 mL). The resulting solution was allowed to react overnight. The acetonitrile was removed under reduced pressure, and the resulting aqueous solution was acidified to pH ca. 2 with concentrated aqueous hydrogen chloride. The resulting precipitate was collected by filtration and washed with water. Purified by recrystallization from water. ^{1}H-NMR (300 MHz, DMSO-d_6): δ (ppm) 2.1 (3H, s, $COCH_3$), 7.7 (2H, d, ArH), 7.9 (2H, d, ArH), 10.3 (1H, s, NH), 12.7 (1H, br s, CO_2H). UV (10^{-2} mol L^{-1} phosphate, pH 7.0): $\lambda_{max} = 262$ nm (ε 1.06×10^4).

2.2. Preparation of 4-(acetylamino)-2-hydroxybenzoic acid (*1b*)

Prepared from 4-amino-2-hydroxybenzoic acid as described for **1a**. Purified by recrystallization from 50% ethyl alcohol in water. ^{1}H-NMR (300 MHz,

DMSO-d_6): δ (ppm) 2.0 (3H, s, $COCH_3$), 7.1 (1H, d, ArH), 7.3 (1H, s, ArH), 7.7 (1H, d, ArH), 10.2 (1H, s, NH), 11.4 (1H, br s, OH), 13.5 (1H, br s, CO_2H). UV (10^{-2} mol L^{-1} phosphate, pH 7.0): $\lambda_{max} = 263$ nm (ε 1.28×10^4); 298 nm (ε 7.56×10^3).

2.3. Preparation of 7-hydroxycoumarin-3-carboxylic acid (**2b**)

Prepared by condensation of 2,4-hydroxybenzaldehyde and diethylmalonate followed by saponification of the resulting ethyl ester (Joule and Mills, 2000). Purified by recrystallization from 95% ethyl alcohol. ^{1}H-NMR (300 MHz, DMSO-d_6): δ (ppm) 6.7 (1H, s, C8-H), 6.9 (1H, d, C6-H), 7.7 (1H, d, C5-H), 8.7 (1H, s, C4-H), 12.0 (1H, br s, OH). UV (10^{-2} mol L^{-1} phosphate, pH 7.0): $\lambda_{max} = 339$ nm (ε 1.62×10^4); 380 nm (ε 6.26×10^3).

2.4. Preparation of 3H-phenoxazin-3-one (**3a**)

Prepared by the oxidation of phenoxazine with ferric chloride (Bolognese et al., 2002). Purified by recrystallization from water.

2.5. Irradiation

Aliquots (10 mL) of solutions containing the unhydroxylated benzoate (**1a**), coumarin (**2a**), or phenoxazine (**3a**) at ca. 10^{-4} mol L^{-1} (except ca. 10^{-6} mol L^{-1} in the case of the less soluble **3a**) in an aqueous phosphate buffer (10^{-2} mol L^{-1}, pH 7.0), and usually one of four radical scavengers (DMSO, methyl alcohol, acetone, or acetonitrile) were irradiated aerobically with ^{137}Cs γ-rays (662 keV) in 15 mL glass test tubes. The maximum radiation dose was 180 Gy. Dose rates were between 2.9×10^{-1} and 1.7×10^{-3} Gy s^{-1}, determined with the Fricke system (Klassen et al., 1999).

2.6. Fluorescence

The fluorescence of the irradiated solutions was measured for an aliquot (3 mL) of each irradiated sample using an Aminco-Bowman instrument with excitation and emission bandwidths both of 5.5 nm. Excitation and emission wavelengths are listed in Table 1. The response was calibrated with solutions of authentic compounds whose concentration had been determined gravimetrically.

Table 1
Excitation and emission wavelengths for the fluorescent compounds shown in Fig. 1

Structure	Excitation (nm)	Emission (nm)
1b	300	350
2b	385	450
3b	570	585

3. Results and discussion

3.1. Chemical species

Fig. 1 shows the chemical structures of the benzoate (**1a**), coumarin (**2a**), and phenoxazinone (**3a**) compounds that we used in this study. The structures of their fluorescent hydroxylated derivatives are also shown (**1b**, **2b**, and **3b**). Only compounds **2a** and **3b** are commercially available, so the others were synthesized from available precursors and characterized spectroscopically. The wavelengths used for the fluorescence detection of compounds **1b**, **2b**, and **3b** are listed in Table 1.

3.2. Formation of fluorescent products by irradiation

The formation of fluorescent products after gamma irradiation of compound **2a** is shown in Fig. 2. There are four typical yield dose plots for the irradiation of 1.03×10^{-4} mol L^{-1} **2a** in the presence of four different concentrations of acetone in the range zero to 2×10^{-2} mol L^{-1}. The emission and excitation wavelengths were respectively 385 and 450 nm. Increasing irradiation dose produces an increase in the fluorescence signal, but the presence of acetone attenuates this dose-dependent response. The slopes of the straight lines fitted to the data in Fig. 2 provide a value for the radiation chemical yield (also called a G value) of the hydroxylated fluorescent product (compound **2b**) at each of the four different concentrations of acetone. The G value for the formation of compound **2b** is symbolized as G(**2b**). The use of the excitation and emission wavelengths determined by using an authentic sample of compound **2b** implies that it was this compound that was being detected as an irradiation product of compound **2a**. Inhibition of the formation of compound **2a** by acetone is consistent with $^{\bullet}$OH scavenging by acetone. Increasing concentrations of acetone are able to compete with increasing effectiveness against the fixed concentration of compound **2a** for $^{\bullet}$OH. Addition of acetone after irradiation but before fluorescence assay did not prevent the formation of fluorescent products (not shown).

3.3. Inhibition of fluorescence formation by additives

Fig. 2 reveals that the presence of acetone during irradiation decreases the yield of the fluorescent product **2b**. If it is assumed that competition for $^{\bullet}$OH between acetone and **2a** is responsible, it is possible to analyze

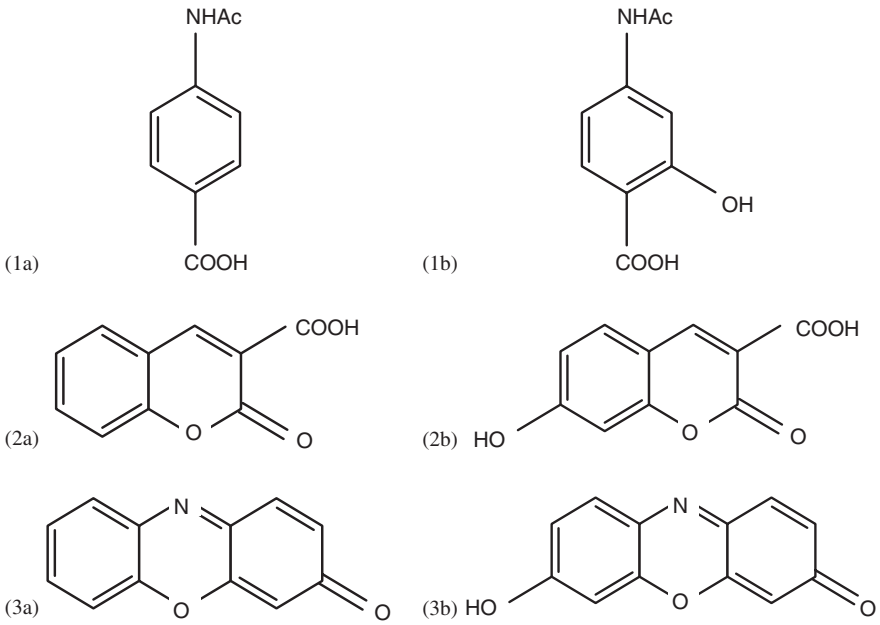

Fig. 1. Chemical structures of the species examined in this study. The names of the compounds are: (**1a**) 4-(acetylamino)benzoic acid; (**1b**) 4-(acetylamino)-2-hydroxybenzoic acid (trivial name 4-(acetylamino)salicylic acid); (**2a**) coumarin-3-carboxylic acid; (**2b**) 7-hydroxycoumarin-3-carboxylic acid (trivial name umbelliferone-3-carboxylic acid); (**3a**) 3H-phenoxazin-3-one; (**3b**) 7-hydroxy-3*H*-phenoxazin-3-one (trivial name resorufin).

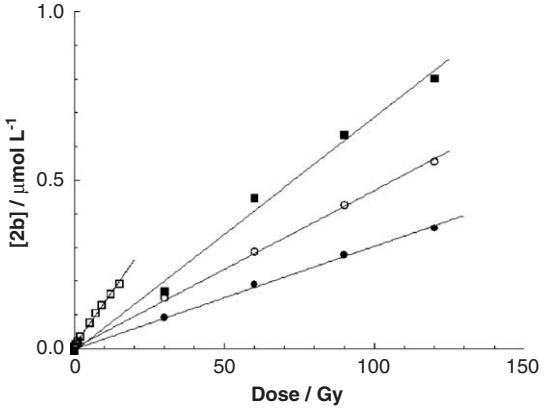

Fig. 2. Formation of fluorescent products after the irradiation of coumarin compound **2a** (1.03×10^{-4} mol L^{-1}). Compound **2a** was irradiated in the presence of one of four different concentrations of acetone. These were zero (open square); 5×10^{-3} mol L^{-1} (closed square); 1×10^{-2} mol L^{-1} (open circle); or 2×10^{-2} mol L^{-1} (closed circle). The four data sets are each fitted with a least mean square straight line of the form $y=mx+c$. From the slopes m of these straight lines, the radiation chemical yields of the fluorescent product **2b** are respectively 12.7, 7.34, 4.81, and 3.19 nmol J^{-1}.

this effect using competition kinetics. The two reactions in competition with one another are the formation of **2b** from **2a** (reaction 1) and the scavenging of $^{\bullet}$OH by acetone (reaction 2). The rate constants of these two reactions are respectively k_1 and k_2.

$$\mathbf{2a}+{}^{\bullet}\mathrm{OH}\rightarrow\mathbf{2b} \quad (1)$$

$$\text{acetone}+{}^{\bullet}\mathrm{OH}\rightarrow\text{Products} \quad (2)$$

This competition may be described quantitatively by Eq. (1).

$$\frac{1}{G(\mathbf{2b})}=\frac{1}{G_0(\mathbf{2b})}+\frac{k_2[\text{acetone}]}{G_0(\mathbf{2b})k_1[\mathbf{2a}]} \quad (1)$$

The yield of **2b** in the absence of any added acetone is symbolized by G_0(**2b**). Eq. (1) is applicable to small radiation doses such that the concentration of **2a** remains essentially constant and much larger than the concentrations of products that are formed. These conditions are fulfilled at under the conditions for the data plotted in Fig. 2, where the concentration of the precursor **2a** is ca. 10^{-4} mol L^{-1} and the fluorescent product is formed in sub-micromolar concentrations. The fit of a straight line to the data plotted in Fig. 3 implies that Eq. (1) is valid. The value of the slope m is equal to k_2c/k_1[**2a**], where c is the intercept. Since a value for k_2 is available in the literature ($k_2=8.5\times10^7$ L mol^{-1} s^{-1}) (Buxton et al., 1988) a value for k_1 may be estimated as $(8.5\times10^7\times0.0806\times10^9)/(11.8\times10^9\times1.03\times10^{-4})=5.6\times10^9$ L mol^{-1} s^{-1}.

The results plotted in Fig. 2 and analyzed in Fig. 3 were repeated with three other scavengers (not shown).

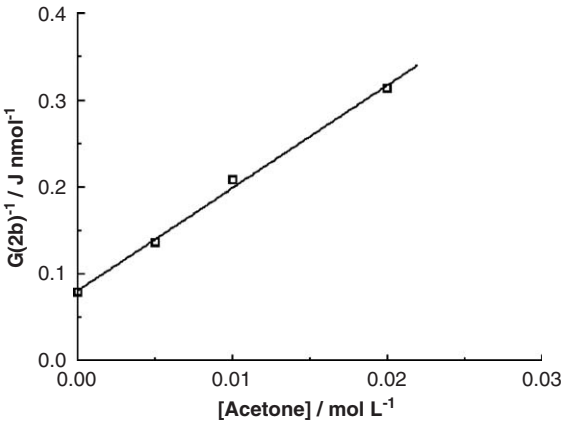

Fig. 3. Formation of fluorescent compound **2b** in the presence of acetone, according to competition kinetics. The yields of compound **2b** were derived from the slopes of the yield dose plots in Fig. 2. The data set is fitted with a least mean square straight line of the form $y = mx + c$. The values of the slope m and intercept c are respectively $11.8 \times 10^9\,\mathrm{J\,dm^3\,mol^{-2}}$ and $0.0806\,\mathrm{J\,nmol^{-1}}$.

Table 2
Rate constants for the formation of the fluorescent products **1b**, **2b**, and **3c** by reaction of $^{\bullet}$OH with the precursors **1a**, **2a**, and **3a**, respectively

Scavenger	Rate constant ($\mathrm{L\,mol^{-1}\,s^{-1}}$)		
	1a + $^{\bullet}$OH	**2a** + $^{\bullet}$OH	**3a** + $^{\bullet}$OH
DMSO	4.3×10^9	5.6×10^9	14×10^9
Methyl alcohol	4.4×10^9	5.5×10^9	15×10^9
Acetone	3.5×10^9	5.6×10^9	9.9×10^9
Acetonitrile	2.6×10^9	2.3×10^9	9.2×10^9

These were DMSO, methyl alcohol, and acetonitrile. Literature values of k_2 are respectively 7.1×10^9, 8.4×10^8, and $5.5 \times 10^6\,\mathrm{L\,mol^{-1}\,s^{-1}}$ (Buxton et al., 1988). The resulting estimates for k_1 are respectively 5.6×10^9, 5.5×10^9, and $2.3 \times 10^9\,\mathrm{L\,mol^{-1}\,s^{-1}}$.

These measurements were repeated for compounds **1a** and **3a**. The resulting estimates of the rate constant for reaction of **1a** and **3a** with $^{\bullet}$OH are listed in Table 2. In general the four estimates for the rate constants are consistent with one another. Rate constants for the reaction of $^{\bullet}$OH with compounds having structures similar to **1a**, **2a**, and **3a** are available in the literature (Buxton et al., 1988). Examples are $5.9 \times 10^9\,\mathrm{L\,mol^{-1}\,s^{-1}}$ for the benzoate ion (similar to **1a**), $2 \times 10^9\,\mathrm{L\,mol^{-1}\,s^{-1}}$ for coumarin (similar to **2a**), and $1.2 \times 10^{10}\,\mathrm{L\,mol^{-1}\,s^{-1}}$ for diphenylamine (similar to **3a**). All of these are consistent with our results.

Table 3
Yields of fluorescent products **1b**, **2b**, and **3b** from their precursors **1a**, **2a**, and **3a**, after irradiation in the absence of any added scavengers

Structure	Yield ($\mathrm{nmol\,J^{-1}}$)	Yield per $^{\bullet}$OH (%)
1b	25.7	9.5
2b	12.7	4.7
3b	30.2	11

This agreement for four different scavengers having rate constants for reaction with $^{\bullet}$OH roughly equally spread over four orders of magnitude implies that it is the hydroxyl radical and not some other species that is responsible for the formation of the fluorescent product.

3.4. Yield of fluorescent products

In the absence of any added scavenger, essentially all $^{\bullet}$OH that escape the spurs go on to react with the substrate (i.e., compound **1a**, **2a**, or **3a**), since it is the only compound present in solution that is reactive with $^{\bullet}$OH. Comparing the yield of the fluorescent product under these conditions with the yield of $^{\bullet}$OH from water radiolysis provides an estimate of the fraction of $^{\bullet}$OH that produce the fluorescent product. For example, for the irradiation of compound **2a**, the yield for the formation of **2b** in the absence of acetone (see Fig. 2) was $12.7\,\mathrm{nmol\,J^{-1}}$. The $^{\bullet}$OH yield under these conditions is $270\,\mathrm{nmol\,J^{-1}}$ (Pimblott and LaVerne, 1998). Therefore the yield of the fluorescent product **2b** is $12.7/270 = 4.7\%$ per $^{\bullet}$OH. The same calculation was made for the other two substrates, and the values are listed in Table 3.

A value for the yield of **2b** per $^{\bullet}$OH reaction with **2a** has been reported previously (Collins et al., 1994) as a G value of 0.123 (in units of $(100\,\mathrm{eV})^{-1}$). This is equivalent to $0.123/(F \times 100) = 12.8\,\mathrm{nmol\,J^{-1}}$ in SI units, where F is Faraday's constant. Although these authors do not report a value for the rate constant of **2a** with $^{\bullet}$OH, they do provide sufficient data to arrive at an estimate of $9.4 \times 10^9\,\mathrm{L\,mol^{-1}\,s^{-1}}$ (based on a competition between DMSO and **2a**). These values compare well with our estimates (see Tables 2 and 3).

3.5. Summary

The substrates we examined here all react rapidly with $^{\bullet}$OH to produce fluorescent products in moderate yield. Therefore it is possible that one or more of these functional groups may form the basis for detecting the $^{\bullet}$OH clusters expected to be formed by ionizing radiation (see Introduction).

Acknowledgements

Supported by PHS Grant CA46295. We thank Chris Sherrill (Department of Chemistry, University of California at San Diego) for assistance with ^{1}H-NMR spectroscopy.

References

Ali, M.A., Yasui, F., Matsugo, S., Konishi, T., 2000. The lactate dependent enhancement of hydroxyl radical generation by the Fenton reaction. Free Radical Res. 32, 429–438.

Bernhard, W.A., Close, D.M., 2003. DNA damage dictates the biological consequences of ionizing irradiation. The chemical pathways. In: Mozumder, A., Hatano, Y. (Eds.), Charged Particle and Photon Interactions with Matter: Chemical, Physicochemical and Biological Consequences with Applications. Marcel Dekker, New York, pp. 431–470.

Biondi, R., Xia, Y., Rossi, R., Paolocci, N., Ambrosio, G., Zweier, J.L., 2001. Detection of hydroxyl radicals by D-phenylalanine hydroxylation. A specific assay for hydroxyl radical generation in biological systems. Anal. Biochem. 290, 138–145.

Bolognese, A., Correale, G., Manfra, M., Lavecchia, A., Mazzoni, O., Novellino, E., Barone, V., Pani, A., Tramontano, E., La Colla, P., Murgioni, C., Serra, I., Setzu, G., Loddo, R., 2002. Antitumor agents. 1. Synthesis, biological evaluation, and molecular modeling of 5*H*-pyrido[3,2-a]phenoxazin-5-one, a compound with potent antiproliferative activity. J. Med. Chem. 21, 5205–5216.

Bottle, S.E., Hanson, G.R., Micallef, A.S., 2003. Application of the new EPR spin trap 1,1,3-trimethylisoindole *N*-oxide (TMINO) in trapping $HO^{\bullet}$ and related biologically important radicals. Org. Biomol. Chem. 1, 2585–2589.

Buxton, G.V., Greenstock, C.L., Helman, W.P., Ross, A.B., 1988. Critical review of rate constants for reactions of hydrated electrons, hydrogen atoms, and hydroxyl radicals ($^{\bullet}OH/^{\bullet}O^{-}$) in aqueous solution. J. Phys. Chem. Ref. Data 17, 513–886.

Collins, A.K., Makrigiorgos, G.M., Svensson, G.K., 1994. Coumarin chemical dosimeter for radiation therapy. Med. Phys. 21, 1741–1747.

Fulford, J., Nikjoo, H., Goodhead, D.T., O'Neill, P., 2001. Yields of SSB and DSB induced in DNA by Al(K) ultrasoft X-rays and alpha particles. Comparison of experimental and simulated yields. Int. J. Radiat. Biol. 77, 1053–1066.

Gutteridge, J.M., Halliwell, B., 2000. Free radicals and antioxidants in the year 2000. A historical look at the future. Ann. N. Y. Acad. Sci. 899, 136–147.

Ivan, M.G., Scaiano, J.C., 2003. A new approach for the detection of carbon centered radicals in enzymatic processes using prefluorescent probes. Photochem. Photobiol. 78, 416–419.

Joule, J.A., Mills, K., 2000. Heterocyclic Chemistry, fourth ed. Blackwell Science, Oxford, UK.

Klassen, N.V., Shortt, K.R., Seuntjens, J., Ross, C.K., 1999. Fricke dosimetry. The difference between G(Fe^{3+}) for ^{60}Co gamma rays and high energy X-rays. Phys. Med. Biol. 44, 1609–1624.

Li, B., Gutierrez, P.L., Blough, N.V., 1997. Trace determination of hydroxyl radical in biological systems. Anal. Chem. 69, 4295–4302.

Liu, M., Liu, S., Peterson, S.L., Miyake, M., Liu, K.J., 2002. On the application of 4-hydroxybenzoic acid as a trapping agent to study hydroxyl radical generation during cerebral ischemia and reperfusion. Mol. Cell. Biochem. 234–235, 379–385.

Lundqvist, M.J., Eriksson, L.A., 2000. Hydroxyl radical reactions with phenols as a model for generation of biologically reactive tyrosyl radicals. J. Phys. Chem. B 104, 848–855.

Manevich., Y., Held, K., Biaglow, J.E., 1997. Coumarin-3-carboxylic acid as a detector for hydroxyl radicals generated chemically and by gamma radiation. Radiat. Res. 148, 580–591.

Milligan, J.R., Ward, J.F., 1994. Yield of single strand breaks due to attack on DNA by scavenger derived radicals. Radiat. Res. 137, 295–299.

Milligan, J.R., Ng, J.Y.-Y., Wu, C.C.L., Aguilera, J.A., Ward, J.F., Kow, Y.W., Wallace, S.S., Cunnigham, R.P., 1996. Methylperoxyl radicals as intermediates in the damage to DNA irradiated in aqueous dimethyl sulfoxide with gamma rays. Radiat. Res. 146, 436–443.

Nakamura, K., Hanna, I.H., Cai, H., Nishimura, Y., Williams, K.M., Guengerich, F.P., 2001. Coumarin substrates for cytochrome P450 2D6 fluorescence assays. Anal. Biochem. 292, 280–286.

Pimblott, S.M., LaVerne, J.A., 1998. Effect of electron energy on the radiation chemistry of liquid water. Radiat. Res. 150, 159–169.

Saran, M., Summer, K.H., 1999. Assaying for hydroxyl radicals. Hydroxylated terephthalate is a superior fluorescence marker than hydroxylated benzoate. Free Radical Res. 31, 429–436.

Selvin, P.R., 2000. The renaissance of fluorescence resonance energy transfer. Nature Struct. Biol. 7, 730–734.

Shen, M.Q., Yun, S., Tao, Q.Y., 1995. Synthesis of fluoran dyes with improved properties. Dyes Pigments 29, 45–55.

Soh, N., Makihara, K., Sakoda, E., Imato, T., 2004. A ratiometric fluorescent probe for imaging hydroxyl radicals in cells. Chem. Commun. 7, 496–497.

Villegas, M.L., Bertolotti, S.G., Previtali, C.M., Encinas, M.V., 2005. Reactions of excited states of phenoxazin-3-one dyes with amino acids. Photochem. Photobiol. 81, 884–890.

Watrob, H.M., Pan, C.P., Barkley, M.D., 2003. Two step FRET as a structural tool. J. Am. Chem. Soc. 125, 7336–7343.